KAON AND PION INTERFEROMETRY FROM NA44

Sanjeev U. Pandey, Ohio State University, Columbus, OH 43212, USA.

Abstract

Kaon and pion correlations from S+Pb collisions at 200 GeV/c per nucleon and p+Pb collisions at 450 GeV/c are presented. Multi-dimensional fits are performed to characterize the kaon emission volume which is found to be smaller than fits to the pion emission volume. Further, the p_T dependance of pion correlations are studied.

1 Introduction

Two-particle intensity interferometry provides a method for measuring the space–time extent of a particle-emitting source when the emitted radiation is at least partially incoherent [1, 2, 3]. Intensity interferometry measures the freeze-out volume when the particles decouple from the source. This effect is well established for pions. Charged kaons are less affected by resonance decay than pions and could provide a cleaner signal of the source [4, 5]. Furthermore, the different total cross sections of K^+, K^-, and π^+ with nuclear matter may allow one to investigate the source at different decoupling times [6].

Experiment NA44 is optimized for the study of identified single- and two-particle distributions at mid-rapidity. Excellent particle identification limits contamination to the 1% level. Since it is a focusing spectrometer the acceptance for pairs of particles with small momentum difference is optimized allowing small statistical uncertainties in the two-particle correlation function in the region of the signal from Bose–Einstein correlations. The RQMD event generator[7], which simulates heavy ion collisions, predicts that $\approx$ 34% of pions with p_T less than 200 GeV/c, $\approx$ 10% of pions with p_T larger than 200 GeV/c and $\approx$ 5% of K's near mid-rapidity ($2 < y < 4$) come from the decay of resonances with lifetimes $c\tau > 20$fm.

2 Experimental Setup

The focusing spectrometer of the NA44 experiment has been described in detail elsewhere[8]. Two dipole magnets and three quadrupoles create a magnified image of the target in the spectrometer. Only one charge sign can be detected in the spectrometer at a time. The beam rate and time-of-flight start signal are determined using a Cherenkov beam counter for Sulphur beam and a forward scintillator counter for proton beam. A silicon pad detector is used to measure the charged-particle multiplicity distribution with 2π azimuthal acceptance in the pseudorapidity range $1.5 < \eta < 3.3$.

The spectrometer uses three highly segmented scintillator hodoscopes, for tracking and time-of-flight measurements. In this analysis we use the time measured between the last hodoscope and the start counter for particle identification. The total time resolution is approximately 100 ps. Threshold

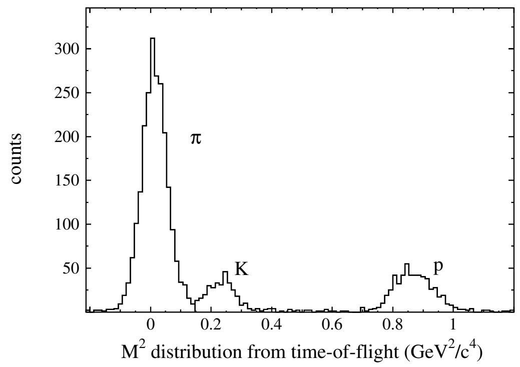

Figure 1: Mass squared plots.

Cherenkov detectors also provide particle identification and a fast trigger.

3 Data Analysis

Tracks are reconstructed from hit positions on the three hodoscopes, with pattern recognition constrained by straight-line trajectories after the magnets. Figure 1 shows the distribution of the mass-squared calculated from measured momentum and time-of-flight in S + Pb collisions. Well separated pions, kaons and protons are visible. Contamination of pairs by tracks not originating at the target is less than 3%.

Data are analyzed in a 3-dimensional coordinate frame. The direction parallel to the beam, Q_l, and the direction perpendicular to the beam which may be further resolved into a direction along the momentum sum of the particles, Q_{to} and perpendicular to this, Q_{ts}. Here $q_i = k_{1,i} - k_{2,i}$ and k_i are the particle momenta. Being parallel to the velocities of the particles, Q_{to} is sensitive to the lifetime of the source [9]. Data are analyzed in the frame in which the momentum sum in the beam direction of both particles is zero. This frame complicates the interpretation of Q_l, however, it decouples the lifetime information from Q_{ts}[9]. The resolution for two particles in Q_{ts} and Q_{to} is about 20 MeV/c and in Q_l is 10 MeV/c. Bins of size 20 MeV/c are used to decrease statistical errors.

The method used to determine the correlation function has been described

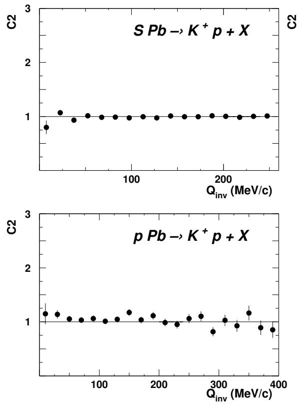

Figure 2: The pK^+ and p^-K^- correlation plots from the horizontal setting assuming both are kaons. The lines are to guide the eye. Error bars are statistical.

in detail elsewhere[8]. The data are fit with:

$$C(Q_{to}, Q_{ts}, Q_L) = D(1 + \lambda e^{-Q_{to}^2 R_{to}^2 - Q_{ts}^2 R_{ts}^2 - Q_L^2 R_L^2}) \tag{1}$$

We use the method of Least-Squares to find the values of the unknown parameters and minimize the statistic

$$\chi^2 = \sum_{i,j} (C_i - A_i/B_i) V_{ij}^{-1} (C_j - A_j/B_j) \tag{2}$$

where V_{ij} is the covariance matrix defined below and one sums over bins (i, j) where there are more than 10 counts in the 'reals' (A_i) distribution. This affects bins at high Q at the edge of our acceptance. Maximum likelihood estimators reduce to Least-Square estimators in this limit.

Systematic errors are evaluated by varying analysis parameters and seeing the difference in the correlation functions produced. The error matrix is calculated from

$$V_{ij}^{sys} = \left[\frac{\sum_{k=1}^{N} C_{ik} C_{jk}}{N} - C_i^{mean} C_j^{mean}\right] \frac{N}{N-1} \tag{3}$$

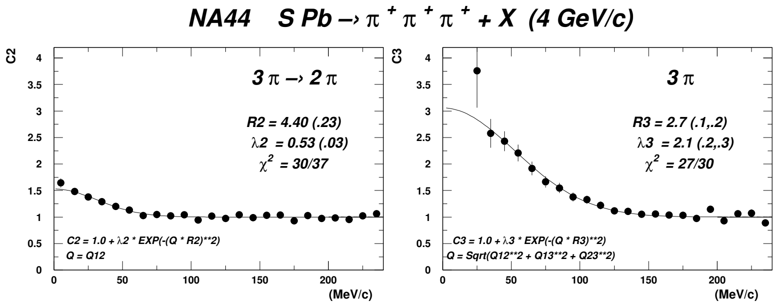

$\lambda 3 = 3*\lambda 2 + 2*\lambda 2^{1.5}$ $R2^2/3 < R3^2 < R2^2/2$

$2.1\ (.4) = 2.4\ (.2)$ $6.45\ (.67) < 7.3\ (1.1) < 9.68\ (1.01)$

Figure 3: Comparison of correlations of two pions with correlations of three pions.

where N equals the number of simulated data sets and $V_{ij} = V_{ij}^{sys} + V_{ij}^{stat}$, $V_{ij}^{stat} = 0$ if $i \neq j$. For our data the correlation coefficient $\rho_{ij} = V_{ij}/(V_{ii}V_{jj})^{\frac{1}{2}}$ is less than 0.2 for almost all bins indicating that the systematic errors have little effect on fits to the data.

No correction for the 1% contamination of the data sets by Kp events or $K\mu$ events is made.

4 Results

To investigate the effect of the 1% contamination of the KK data set by Kp, a correlation is constructed from Kp pairs assuming both are kaons. As expected the correlations are flat as seen in Figure 2.

Three particle interferometry can serve as a self-consistent check on one's data analysis by comparisons to two particle interferometry[10]. The data

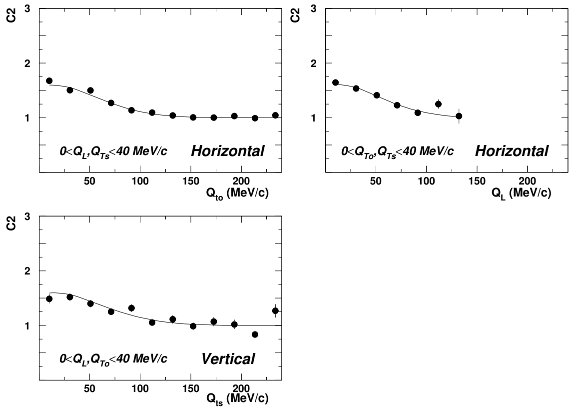

Figure 4: The Q_{to}, Q_{ts} and Q_l projections for $S+Pb \rightarrow K^+K^+ + X$ collisions. The lines are from a gaussian fit. Error bars are statistical.

are consistent with the pair data as seen from the pictures and equations in Figure 3. There are no data points below ≈ 40 MeV/c as enforcing a distance of one slat between each track on each hodoscope depletes this region while increasing the purity of the three pion sample.

The results from three dimensional fits for Sulphur projectile collisions are summarized in Table 1 and a typical projection of the data onto the three axis are presented in Figure 4. Results for proton projectile collisions are summarized in Table 2.

Table 1: Fitted results of Gaussian parametrizations in Q_{t_o}, Q_{t_s} and Q_l for Sulphur projectile collisions. Results are preliminary.

System	λ	R_{to} (fm)	R_{ts} (fm)	R_l (fm)	χ^2/N_{dof}	$\langle p_T \rangle$
$SPb\ \pi^+\pi^+$	0.56 ± 0.02	4.0 ± 0.1	4.1 ± 0.3	4.7 ± 0.3	1201/1415	150 MeV/c
$SPb\ \pi^+\pi^+$	0.55 ± 0.02	3.0 ± 0.2	3.0 ± 0.2	3.1 ± 0.2	1500/1095	450 MeV/c
$SPb\ K^+K^+$	0.82 ± 0.04	2.8 ± 0.1	2.6 ± 0.2	3.0 ± 0.2	925/1011	250 MeV/c
$SPb\ K^+K^+$	0.83 ± 0.06	3.1 ± 0.2	2.4 ± 0.4	3.4 ± 0.3	258/293	160 MeV/c
$SPb\ K^-K^-$	0.99 ± 0.13		$\approx 2.7 \pm 0.3$			230 MeV/c
$SPb\ \pi^-\pi^-$	0.65 ± 0.03		$\approx 3.9 \pm 0.2$			140 MeV/c

Table 2: Fitted results of Gaussian parametrizations in Q_{t_o}, Q_{t_s} and Q_l for proton projectile collisions. Results are preliminary.

System	λ	R_{to} (fm)	R_{ts} (fm)	R_l (fm)	χ^2/N$_{dof}$	$\langle p_T \rangle$
$pPb\ \pi^+\pi^+$	0.41 ± 0.02	1.9 ± 0.1	2.0 ± 0.3	2.3 ± 0.4	1111/1152	150 MeV/c
$SPb\ K^+K^+$	0.70 ± 0.07	1.5 ± 0.2	1.2 ± 0.8	2.4 ± 0.3	119/121	250 MeV/c

5 Discussion

The similarity of the $\pi^+\pi^+$ and $\pi^-\pi^-$ fit parameters indicate that Coulomb effects on the correlation function by excess single charged particles such as protons are not significant in S+Pb collisions. The similarity of the K^+K^+ and K^-K^- fit parameters is surprising, indicating that different interaction cross sections with nucleons is not important in the central rapidity region at SPS energies. Our measurements show that the p/π^+ ratio is only 0.12,[11] so $K - \pi$ scattering dominates, and is similar for K^+ and K^-. Indeed, in RQMD simulations[7] the average K^+ interacts 1.4 times before freeze out, and K^- 1.0 times. The statistical error on these numbers is approximately 0.3, indicating no significant difference between K^+ and K^- interactions.

We note that the ratio of $K - \pi$ to $\pi - \pi$ cross sections is temperature dependent, and in the range of temperatures likely to be encountered in our experiment they are quite similar.[12] Consequently we might expect similar freeze out radii, but if resonance contributions are greater for pions, the resonance lifetimes will increase the measured radius parameters. The R_{ts} parameter extracted from kaons is smaller than that from our lower p_T pion data sample as seen in Table 1; this is also true for samples of pions and kaons selected to have the same p_T. Our higher p_T pion data which is less diluted from resonance contributions shows similar radii parameters as the kaons.

Another effect of the resonances is to decrease the magnitude of the correlations at low Q, giving us a direct handle on the resonance contributions via the parameter lambda. We find λ_π for our lower p_T data set about 2/3 of λ_K indicating a smaller resonance effect with kaons. However, the λ parameter shows no increase with p_T as expected from this scenario.

In p-Pb collisions it is natural to expect in the central region little rescattering, thermalization, or collective motion, so the transverse motion should be very different from that along the beam. Indeed we see that R_l is quite different from R_{to} and R_{ts}. In S-Pb collisions the three R-parameters are nearly equal, suggesting that the special significance of the beam direction has been reduced by thermalization and collective motion. Furthermore, in p-Pb collisions R_{ts} is similar for kaons and pions, whereas in S-Pb collisions R_{ts} is quite different in the two cases. The simplest way to interpret the R-parameters in terms of the source size would be to compare the size of the projectile nucleus to the measured R_{ts}. Since the nucleus is best described as a hard sphere of constant density, one should fit the correlation data with a hard sphere form rather than a Gaussian. One then finds an experimental R_{ts} (hard sphere) equals 5.7 fm for kaons and 7.1 fm for the lower p_T pions as compared to r(sulphur) = 3.8 fm. It is less clear which projectile size to choose for a p-Pb collision, but if we were to use r(proton) = 1 fm, we would reach a similar conclusion.

6 Conclusions

We have investigated K^+ and K^- correlation functions at mid-rapidity and found them to be similar, indicating a nucleon-free central region in our collisions. Extracted radius parameters for kaons are smaller than those for pions; though resonance decays to pions can in part account for this difference as suggested by the p_T dependance of the pion radius parameters. The radius parameters we measure for $S + Pb$ and $p + Pb$ collisions are both larger than the projectile signaling the presence of collective expansion. Further, radii extracted for pions and kaons are similar for $p + Pb$ collisions indicating little rescattering in these collisions.

7 Acknowledgements

The NA44 Collaboration wishes to thank the staff of the CERN PS-SPS accelerator complex for their excellent work. We thank the technical staff at CERN and the collaborating institutes for their valuable contribution. We are also grateful for the support given by the Science Research Council of Denmark; the Japanese Society for the Promotion of Science, and the Ministry of Education, Science and Culture, Japan; the Science Research Council of Sweden; the US Department of Energy; and the National Science Foundation (Nuclear Physics) through grants PHY8906284 and PHY8958491.

References

[1] R. Hanbury-Brown and R. Q. Twiss, Nature **178** (1956) 1046.

[2] M. Gyulassy, S. K. Kauffmann, and L. W. Wilson, Phys. Rev. **C20** (1979) 2267.

[3] B. Lorstad, Int. J. Mod. Phys. **A4** (1988) 2861.

[4] M. Gyulassy and S. Padula, Phys. Rev. **C41** (1990) 21.

[5] S. Pratt, P. J. Siemens, and A. P. Vischer, Phys. Rev. Lett. **68** (1992) 1109.

[6] S. Schnetzer et al., Phys. Rev. Lett. **49** (1982) 989.

[7] H. Sorge, H. Stöcker, and W. Greiner, Nucl. Phys. **A498** (1989) 567.

[8] H. Beker et al., Phys. Lett. **B302** (1993) 510.

[9] S. Pratt, T. Csörgő, and J. Zimányi, Phys. Rev. **C42** (1990) 2646.

[10] Y. Liu et al., Phys. Rev. **C34** (1986) 1667.

[11] M. Murray et al., Nucl. Phys. **A566** (1994) 515c.

[12] K. Haglin and S. Pratt, Phys. Lett. B in press.

[13] H. Beker et al., Directional analysis of identified pion interferometry at the cern sps, to be published.